

Calibration of a pH sensitive buried channel silicon-on-insulator MOSFET for sensor applications

B. Ashcroft¹, B. Takulapalli², J. Yang², G. M. Laws^{*,2}, H. Q. Zhang^{2,3}, N. J. Tao^{2,3}, S. Lindsay¹, D. Gust⁴, and T. J. Thornton^{2,3}

¹ Department of Physics & Astronomy, P.O. Box 871504, Arizona State University, Tempe, AZ 85287, USA

² Center for Solid State Electronics Research, P.O. Box 876206, Arizona State University, Tempe, AZ 85287, USA

³ Department of Electrical Engineering, P.O. Box 875706, Arizona State University, Tempe, AZ 85287, USA

⁴ Department of Chemistry & Biochemistry, Arizona State University, Tempe, AZ 85287, USA

Received 1 March 2004, accepted 31 May 2004

Published online 28 July 2004

PACS 68.08.–p, 81.07.Pr, 85.30.Tv

The threshold voltage characteristics of a buried channel silicon-on-insulator MOSFET is examined in solutions of varying acidity. Experiments utilizing an integrated micro-fluidic channel exhibit a variation in threshold voltage that appears approximately linear with pH in the range from pH 4 to pH 7, with a sensitivity of ~1 V per pH unit. Charge configuration changes in the vicinity of the MOSFET inversion layer due to protonation/deprotonation of the device surface is proposed as an explanation for the observed shifts in threshold voltage. When the pH range is expanded we observe a non-linear relationship between pH and the threshold voltage of the device, this behavior is explained in terms of deprotonation of the different species of the native oxide surface. Numerical simulations of the MOSFET demonstrate that the threshold voltage sensitivity corresponds to an additional surface positive fixed charge density of $\sim 1 \times 10^{10} \text{ cm}^{-2}$ for each pH unit.

© 2004 WILEY-VCH Verlag GmbH & Co. KGaA, Weinheim

1 Introduction

Field effect transistors (FETs) sensitive to chemical [1] and/or biological [2] environments can be used for a variety of sensing applications that combine the selectivity of biological systems with the batch manufacturing capabilities of planar microelectronics. Modification of the FET electrical characteristics can be achieved by functionalizing the device surface with an appropriate molecular layer. For example, the current flow in a GaAs transistor can be reduced upon attachment of a single monolayer of dicarboxylic acid [3]. Porphyrin films attached to the metal gate of a MOSFET have demonstrated a clear response to methanol, acetic acid and ethylenediamine [4] and amine-functionalized silicon nano-wires have also been used for real-time detection of protein binding events [5].

We report on a CMOS compatible device that utilizes the electrostatic charge of a molecular species to regulate the current through a silicon-on-insulator (SOI) MOSFET [6]. A substrate bias is applied to the MOSFET to form a buried channel electron inversion layer less than 40 nm from the silicon surface. The proximity of the inversion layer to the surface means it is very sensitive to variations in the surface charge distribution. To investigate the effect of surface charge variation on the electrical characteristics of the SOI MOSFET acidic solutions of varying buffered pH are placed in contact with the device sur-

* Corresponding author: e-mail: gez.laws@asu.edu, Tel.: +1 (480) 965-2405, Fax: +1 (480) 965-8058

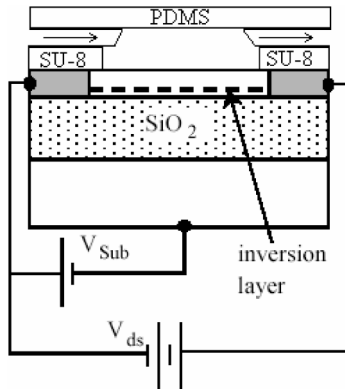


Fig. 1 Schematic cross-section of the pH sensitive MOSFET. A substrate bias, V_{sub} , inverts the lower Si:SiO₂ interface resulting in a buried channel conducting layer which can support a current flowing between the source and drain contacts. The threshold voltage of the buried channel inversion layer is sensitive to the pH of the solution introduced into the micro-fluidic cell on the surface of the device. The micro-fluidic cell consists of a thick layer of patterned photoresist (SU-8) capped with a layer of PDMS. Solutions are injected into the micro-fluidic cell through micro-capillaries as shown by the arrows.

face. The application of differing pH solutions to the FET surface results in a threshold voltage shift of ~ 1 V per pH unit. The threshold voltage shift is simulated by adjusting the fixed charge density on the upper surface of the device as would be expected by the protonation/deprotonation of the amine- and silanol-terminated surface.

2 Device fabrication

The structure of the SOI MOSFET and the integrated micro-fluidic channel is shown in Fig. 1. The device is fabricated from a p-type boron doped (10^{15} cm^{-3}) SOI wafer with an initial silicon channel thickness of 200 nm and a buried oxide (BOX) thickness of 400 nm. The silicon channel is thinned to 150 nm by wet oxidation and the resulting 120 nm of oxide is increased in thickness by Plasma Enhanced chemical vapor deposition (PECVD) to 350 nm. This thick oxide layer is patterned and etched in buffered oxide etch (BOE) as a mask for the source-drain doping. Phosphorous doping is performed in a solid source Tempress diffusion furnace for 30 min at 900 °C. Device isolation is achieved by reactive ion etching (RIE) using SF₆ for 90 seconds. The wafer is then patterned to make holes in the buried oxide for deposition of metal contacts to the substrate silicon, using BOE to etch away the buried oxide from patterned areas. Metal contacts to the substrate and source/drain regions are formed by deposition of 200 nm of aluminum, using a Torr-vac e-beam evaporator. Bonding pads are formed by depositing 10 nm of chromium followed by 100 nm of gold in an Edwards thermal evaporator.

The epoxy based photoresist SU-8 was used to insulate the device from the buffered pH solutions due to its stability in weak acids and bases. A 70 μm thick SU-8 layer was patterned to form an isolated window of 150 $\mu\text{m} \times 500 \mu\text{m}$ above the active region of the device, forming a micro-fluidic cell confining the solutions to the active Si region. After processing the SU-8 layer was hard baked and left permanently on the chip.

A 15 second BOE treatment is used to remove the initial silicon native oxide and a new oxide is allowed to grow under clean-room ambient conditions to a thickness of $\sim 2-3$ nm. In addition to the bare native oxide the common surface modifier aminopropyltriethoxysilane (APTES) was deposited onto the native oxide surface to examine the change in device characteristics between the APTES coated and that of the bare native oxide. A layer of APTES molecules is vapor deposited [X,X], in the presence of the base N,N Di-isopropylethylamine, on the native oxide in an inert atmosphere for 90 minutes. Following the covalent attachment of the APTES to the native oxide the base enables cross linking. The ethoxy group of the APTES undergoes a displacement reaction with SiOH groups on the silicon native oxide, resulting in an $-\text{NH}_2$ surface termination.

After APTES deposition, two capillary tubes (inner diameter 20 μm) were placed on the surface of the SU-8 either side of the active area to form a push-pull fluidic system. Finally, the fluidic system was capped by means of a poly(dimethylsiloxane) (PDMS) mold clamped onto the top of the SU-8 photoresist. The seals formed between the SU-8 and the silicon surface, and between the PDMS cap and the

SU8 and micro-capillaries were sufficiently robust to withstand the pressure applied by the push-pull syringe without leaking.

All acidic solution were made from Tris(hydroxymethyl) aminomethane buffer titrated to the appropriate pH by addition of salt and HCl and tested with litmus paper to determine the final pH.

3 Electrical characterization

The effect of the buffered pH solutions on the SOI MOSFET was evaluated by sweeping the substrate voltage (V_{sub}) and examining changes in the drain current (I_d), before and after altering the solution acidity. The devices were placed in a dark probe station and solutions of various acidity were placed on the active region by means of the push pull pump station. The solutions were strongly buffered to prevent the pH from changing as it traveled down the fused silica tubing, which acts as a competitive pH 6.8 buffer. This competition between the different groups that contact with the solution could be seen as transients in the time evolution of the system to equilibrium and also as increased error bars as the tris buffer was increasingly stressed by the more acidic solutions.

The baseline measurement for comparing drain current characteristics was taken as the device with the APTES surface modification. Figure 2 shows the variation in drain current characteristics for the device with solutions of increasing acidity. If an arbitrary threshold current of 10 nA is assumed then comparing the characteristics of curves in Fig. 2, there is a clear shift in the corresponding threshold voltage towards more negative values with increasing acidity.

In a conventional *n*-channel MOSFET an increase in the concentration of fixed oxide charge would cause such a shift in threshold voltage towards more negative values. An increase in positive fixed oxide charge would result from the protonation of the native oxide surface by the acidic solutions. Protonation of the oxide surface would lead to an increase in positive charge at the surface resulting in an increase in the electron charge density in the device channel. The resulting increase in current would mean the device requires a lower threshold voltage to achieve the same current, as observed in Fig. 2.

If there was a strong effect from the ions in solution we should expect to see strong variations in the slope of the characteristics as the various concentrations of charged ions were moved from the top to the bottom of the SU-8 well under the power of the substrate voltage. The solutions all have a high molar concentration and therefore a Debye screening length of only a few angstroms. This short screening range limits the region of influence to only those charges that are absorbed into the surface layer.

Examination of the inset of Fig. 2 shows an apparent linear relationship between threshold voltage shift and pH rather than the expected titration curve of APTES. This linear behavior could be due to the presence of two different species on the surface of the chip. At low pH values the amine group is proto-

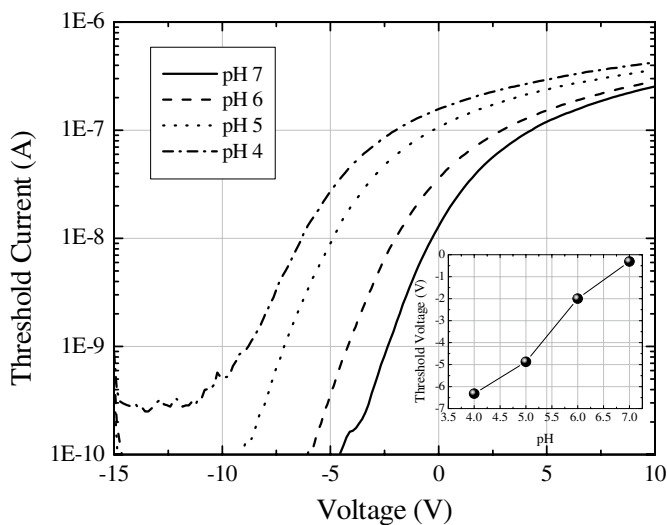


Fig. 2 The drain current as a function of substrate voltage for a fixed drain voltage (V_{ds}) of 10 mV. The curves correspond to pH solutions of 7, 6, 5 and 4. The threshold voltage is defined as that substrate voltage required to produce a drain current of 10 nA and the corresponding voltage at this current is plotted in the inset.

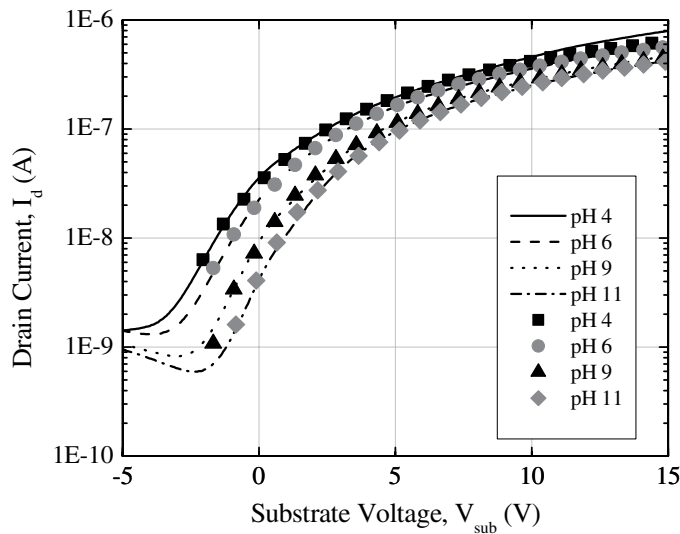


Fig. 3 Drain current versus gate voltage characteristics of the hybrid MOSFET for four different buffered pH solutions. The solid curves denote the experimental data whereas the data point present simulated fits to experimental.

nated to $-\text{NH}_3^+$ whereas at high pH values the silanol groups become $-\text{SiO}^-$ as has been explored by other groups [10]. The competition between these two groups may result in the linear titration curve observed.

To further examine the apparent linear relationship between pH and threshold voltage further devices were prepared and the response of the MOSFET to changes in the surface environment of the exposed oxide was determined by immersing a well-packaged device into static aqueous solutions buffered at different pH values (VWR scientific products). Since there is no significant fluid flow over the device it is assumed that ionic equilibrium is established at the native oxide surface. Figure 3 shows the measured change in drain current as function of back-gate voltage with changing buffer pH (lines). The symbols are derived from a numerical model of the current flow through the device using the device simulator software package Atlas [7]. Again if an arbitrary device threshold current of 10 nA is assumed, then it is clear that the corresponding threshold gate voltage decreases with increasing solution acidity as seen previously with the push-pull pump experiments. It is apparent that threshold voltage magnitudes between the devices in Fig. 2 and Fig. 3 are considerably different and is due to variation in the silicon channel thickness between devices.

The observed threshold voltage shift as a function of the pH for both the bare native oxide and the APTES coated oxide is shown in Fig. 4. The data in Fig. 4 shows that the shift in threshold voltage is

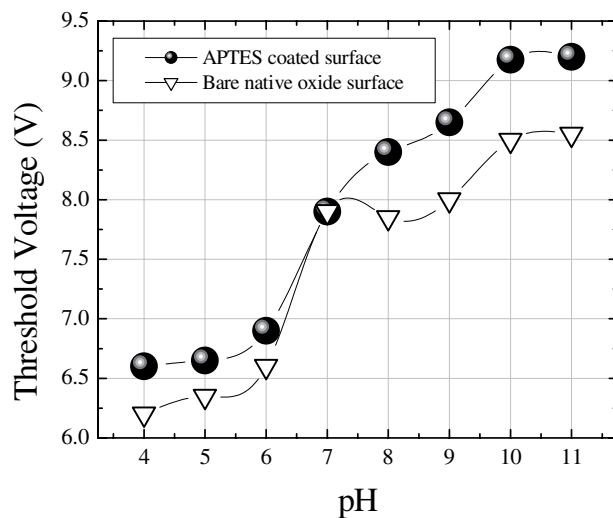


Fig. 4 Threshold voltage shifts as a function of buffered pH value for both the bare native oxide and the APTES coated oxide.

Table 1 Fixed oxide charge and inversion layer mobility data used to obtain simulated electrical data.

| pH | fixed charge density (cm ⁻²) | mobility (cm ² /Vs) |
|----|--|--------------------------------|
| 11 | 8.7×10^{10} | 900 |
| 9 | 1.15×10^{11} | 950 |
| 6 | 1.6×10^{11} | 1100 |
| 4 | 1.82×10^{11} | 1200 |

non-linear over the pH range examined for both the bare native oxide and the APTES coated samples, with small increases in threshold voltage in the pH regions of 6.5 and 9.5. It is speculated the rise in threshold voltage is due to the deprotonation of the single and double silanol groups of the native oxide. The silanol ($\equiv \text{SiOH}$) groups are known to have a pK_a of approximately 6.8 and the disilanol ($= \text{Si}(\text{OH})_2$) are reported to exhibit pK_a values of approximately 9.3 [8]. The APTES surface is reported to have a pK_a of approximately 4 [9], therefore it is expected that the APTES species would be fully deprotonated over the pH range examined and therefore the non-linear behavior observed would be dominated by the native oxide surface due to incomplete surface coverage of the APTES. Further work is on going to examine the role of the different native oxide molecular species on the behavior of the device.

3 Numerical simulations

To further examine the behavior of the devices simulator software package Atlas [7] was used to model the current flowing in the MOSFET. All device dimensions and doping concentrations are based on measured values, except for the thickness of the native oxide, which is taken to be 3 nm. The mobility model used for the simulation takes account of acoustic and optical phonon scattering as well as interface roughness scattering.

The simulations shown in Fig. 3 were achieved by varying the fixed oxide charge at the top native oxide/Si channel interface and also the inversion layer mobility in the silicon channel; these data are shown in Table 1. In order to fit the electrical data shown in Fig. 3 the concentration of interface traps N_{it} was used as a fitting parameter. To obtain a reasonable fit to the data, four trap states at energy levels 0.22, 0.27, 0.32 and 0.4 eV below the conduction band edge were required at densities of 6×10^{10} , 6×10^{10} , 6×10^{10} and $5 \times 10^{10} \text{ cm}^{-2}$, respectively. The traps were assumed to be acceptor-like as expected for trap states in the upper-half of the silicon band gap. Although the assignment of trap energies and densities is somewhat arbitrary, they do follow the general functional form expected for N_{it} [10]. From Table 1, the threshold voltage shift of 2.4 V from pH 11 to pH 4 is brought about by the addition of $9.5 \times 10^{10} \text{ cm}^{-2}$ of positive fixed oxide charge at the top interface.

The charge distribution at the bonding interface between the buffered pH solution and the silicon native oxide depends on the relative magnitudes of the dissociation constant, pK_a , for the native oxide and the solution. The pK_a is a measure of the acidity of a material, similar to pH. For bulk SiO_2 the value of pK_a is ~ 6.8 . When the pH of the solution is lower than that of the native oxide surface adsorption of the acid onto the oxide is expected to result in the protonation of the SiO_2 surface; i.e. more positive charge is present.

4 Conclusions

In conclusion we have shown that the electrical response of a back-gated SOI MOSFET to changes in pH can be described in terms of protonation/deprotonation of the surface species of the silicon native oxide surface. The differences observed for the linear and non-linear relationships between pH and threshold voltage for the micro-fluidic experiments and the static fluid experiments is attributed to differences in equilibrium flow between the two measurements and the ensuing errors involved. The non-linear electrical response to changes in acidity is attributed to the deprotonation of single and double silanol groups for both the bare native oxide and the APTES treated sample due to incomplete APTES surface coverage and complete deprotonation of the APTES in the pH range examined.

Acknowledgements This work is supported by the National Science Foundation (award # ECS-0097434 and CHE-0352599).

References

- [1] J. M. Yang, L. de la Garza, T. J. Thornton, M. Kozicki, and D. Gust, *J. Vac. Sci. Technol. B* **20**, 1706 (2002).
- [2] G. F. Blackman, *Biosensors: Fundamentals and Applications* (Oxford University Press, Oxford, 1987).
- [3] K. Gartsman, D. Cahen, A. Kadyshvitch, J. Libman, T. Moav, R. Naaman, A. Shanzer, V. Umansky, and A. Vilan, *Chem. Phys. Lett.* **283**, 301 (1998).
- [4] M. Andersson, M. Holmberg, I. Lundstrom, A. Lloyd-Spetz, P. Martensson, R. Paolesse, C. Falconi, E. Proietti, C. Di Natale, and A. D'Amico, *Sens. Actuators B* **77**, 567 (2001).
- [5] Y. Cui, Q. Q. Wei, H. K. Park, and C. M. Lieber, *Science* **293**, 1289 (2001).
- [6] G. M. Laws, T. J. Thornton, J. M. Yang, L. De la Garza, M. Kozicki, and D. Gust, *phys. stat. sol. (b)* **233**, 83 (2002).
- [7] ATLAS Device Simulation Framework, SILVACO International, Santa Clara (2000).
- [8] L. H. Allen and E. Matijevi, *J. Colloid Interf. Sci.* **33**, 420 (1970).
- [9] D. V. Vezenov, A. Noy, L. F. Rozsnyai, and C. M. Lieber, *J. Am. Chem. Soc.* **119**, 2006 (1997).
- [10] E. H. Nicollian and J. R. Brews, *MOS Physics and Technology* (Wiley, New York, Chichester, 1982).